CHEMISTRY
A European Journal

Supporting Information

High-Resolution 3D Proton MRI of Hyperpolarized Gas Enabled by Parahydrogen and Rh/TiO_2 Heterogeneous Catalyst

Kirill V. Kovtunov,*[a] Danila A. Barskiy,[a] Aaron M. Coffey,[b] Milton L. Truong,[b] Oleg G. Salnikov,[a] Alexander K. Khudorozhkov,[c] Elizaveta A. Inozemtseva,[c] Igor P. Prosvirin,[c] Valery I. Bukhtiyarov,[c] Kevin W. Waddell,[b] Eduard Y. Chekmenev,*[b] and Igor V. Koptyug[a]

chem_201403604_sm_miscellaneous_information.pdf
chem_201403604_sm_v1_vu_gas.avi
chem_201403604_sm_v2_vu-water.avi

Catalysts preparation and characterization

Commercially available $RhCl_3{}^*3H_2O$ was used as the precursor for rhodium catalyst preparation. The catalysts samples were prepared via wet impregnation of TiO_2 support (Hombifine, S_{BET}=200 m^2/g; dried at 120 °C for 2 hours) with $Rh(NO_3)_3$ aqueous solution. Two different methods of rhodium nitrate solution preparation were used to study the influence of the precursor nature on the dispersion of rhodium particles in Rh supported catalysts. According to the first approach, rhodium iodide was prepared by the precipitation of $RhCl_3$ with KI, and then rhodium nitrate was prepared by dissolving rhodium iodide in nitric acid with simultaneous reduction of iodide ions by hydrogen peroxide (Rh_nI^-).[1] In another approach, rhodium nitrate (III) solutions with varying relative concentrations of nitric acid and Rh were used. The starting material for the preparation of nitrate solutions according to this procedure was $Rh(OH)_3$ which was prepared by precipitation of $RhCl_3$ with sodium hydroxide at pH = 10.5 (Rh_nOH^-). Next, both rhodium nitrate solutions (Rh_nI^- and Rh_nOH^-) were used for the supported rhodium catalysts preparation. To determine the influence of temperature treatment on the active component dispersion level, the reduction of samples under the hydrogen flow at 300 °C for 3 hours with calcination at different temperatures (400 °C for 4 hours, 600 °C for 2 hours) and without preliminary calcination step was performed.

X-Ray Photoelectron spectra (XPS) were recorded using SPECS spectrometer with PHOIBOS-150-MCD-9 hemispherical energy analyzer (Al K_α, irradiation, hν = 1486.6 eV, 200 W). The samples were supported onto double-sided conducting copper scotch tape. Binding energy (BE) scale was preliminarily calibrated by the position of the peaks of $Au4f_{7/2}$ (BE = 84.0 eV) and $Cu2p_{3/2}$ (BE = 932.67 eV) core levels. The binding energies of peaks were calibrated by the position of the C1s peak (BE = 284.8 eV) corresponding to the surface hydrocarbon-like deposits (C-C and C-H bonds). The survey spectra were recorded at pass energy of the analyzer of 50 eV, while that for the narrow spectral regions was 10 eV. Pt, Rh and Pd foils were used as reference materials. The Pt4f, Rh3d and Pd3d peaks in the foils and Pt/TiO_2, Rh/TiO_2 and Pd/TiO_2 catalysts were measured at the same experimental conditions.

Figure S1 (a) presents Pt4f core-level spectra obtained for Pt/TiO_2, TiO_2 used as a support, the difference between these two spectra, and the spectrum of platinum foil as the reference. Rh3d core-level spectra obtained for Rh/TiO_2 catalyst and for rhodium foil as the reference are shown in Fig. S1 (b). Fig.S1 (c) presents Pd3d core-level spectra obtained over Pd/TiO_2 catalyst and palladium foil as the reference. The $Pt4f_{7/2}$ peak at 71.2 eV (difference spectrum), $Rh3d_{5/2}$ peak at 307.2 eV and $Pd3d_{5/2}$ peak at 335.1 eV observed in corresponding supported samples can be attributed to metallic Pt, Rh and Pd, respectively.

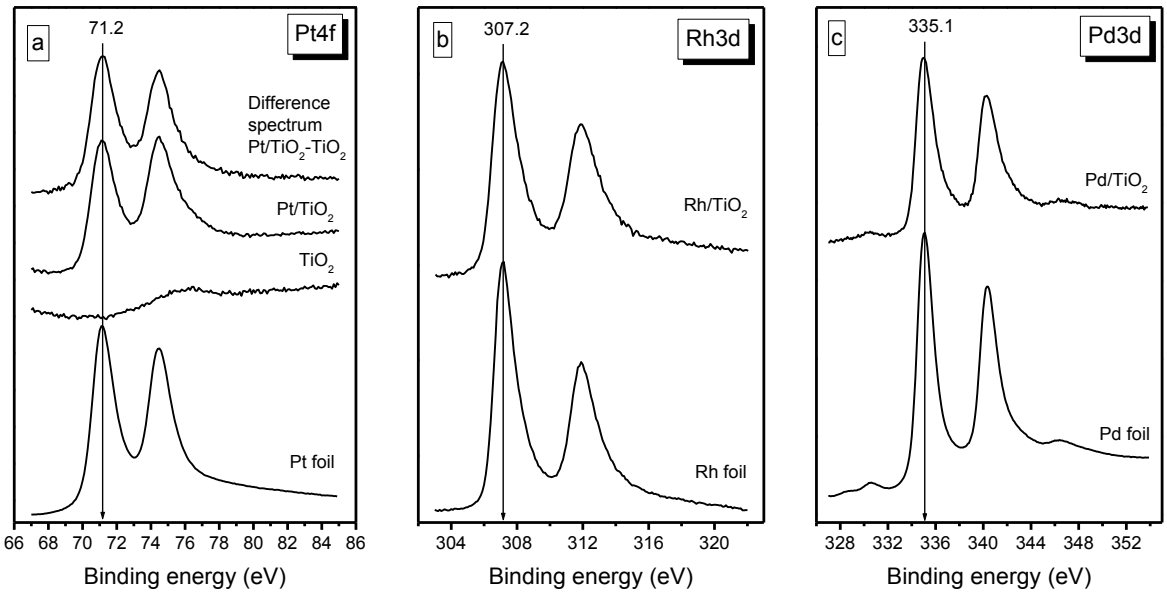

Figure S1. The Pt4f, Rh3d and Pd3d XPS spectra of studied samples: a) Pt/TiO_2, TiO_2 and Pt foil, b) Rh/TiO_2 and Rh foil, and c) Pd/TiO_2 and Pd foil.

Transmission electron microscopy (TEM) (model number JEM-2010, Jeol Co.) (Fig. S2) and CO chemisorption were used to characterize the mean particle size and dispersion of active component.

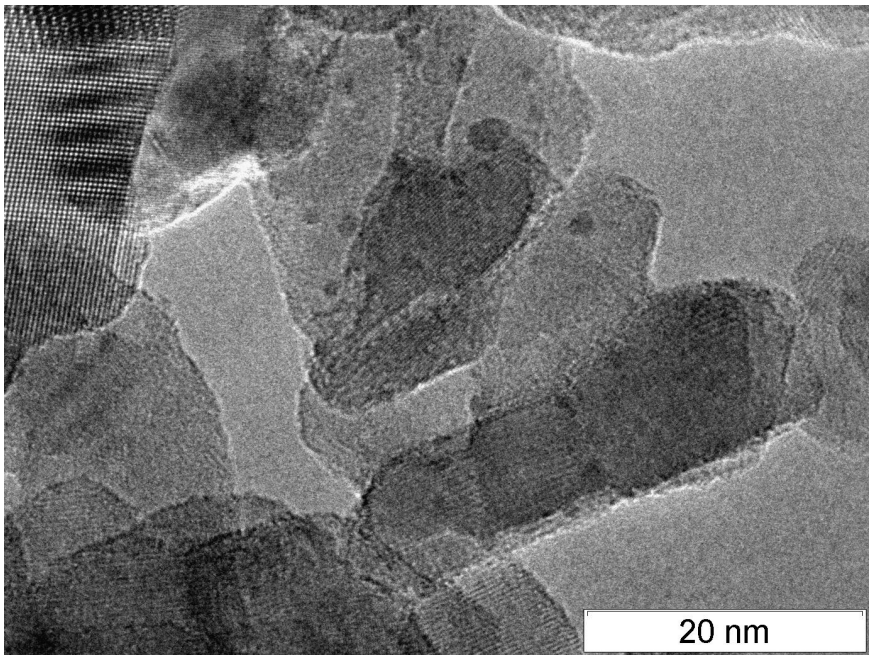

Figure S2. A representative TEM image of Rh/TiO_2 catalyst.

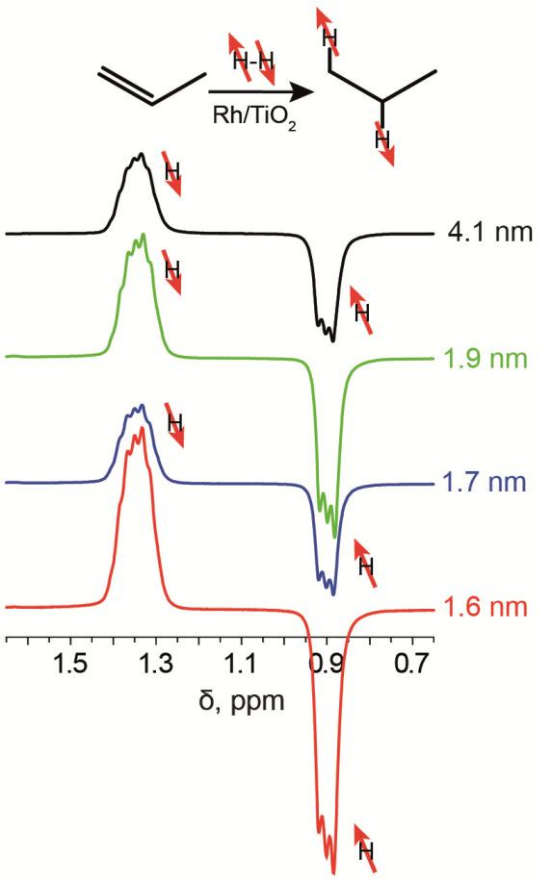

Figure S3. Proton NMR spectra of hyperpolarized propane gas detected in an ALTADENA experiment.[3] The spectra are acquired on a 9.4 T high-resolution NMR spectrometer during heterogeneous hydrogenation of propene to propane with parahydrogen over Rh/TiO_2 catalysts with different metal particles sizes. The experimental setup shown in Fig. 1a was used.

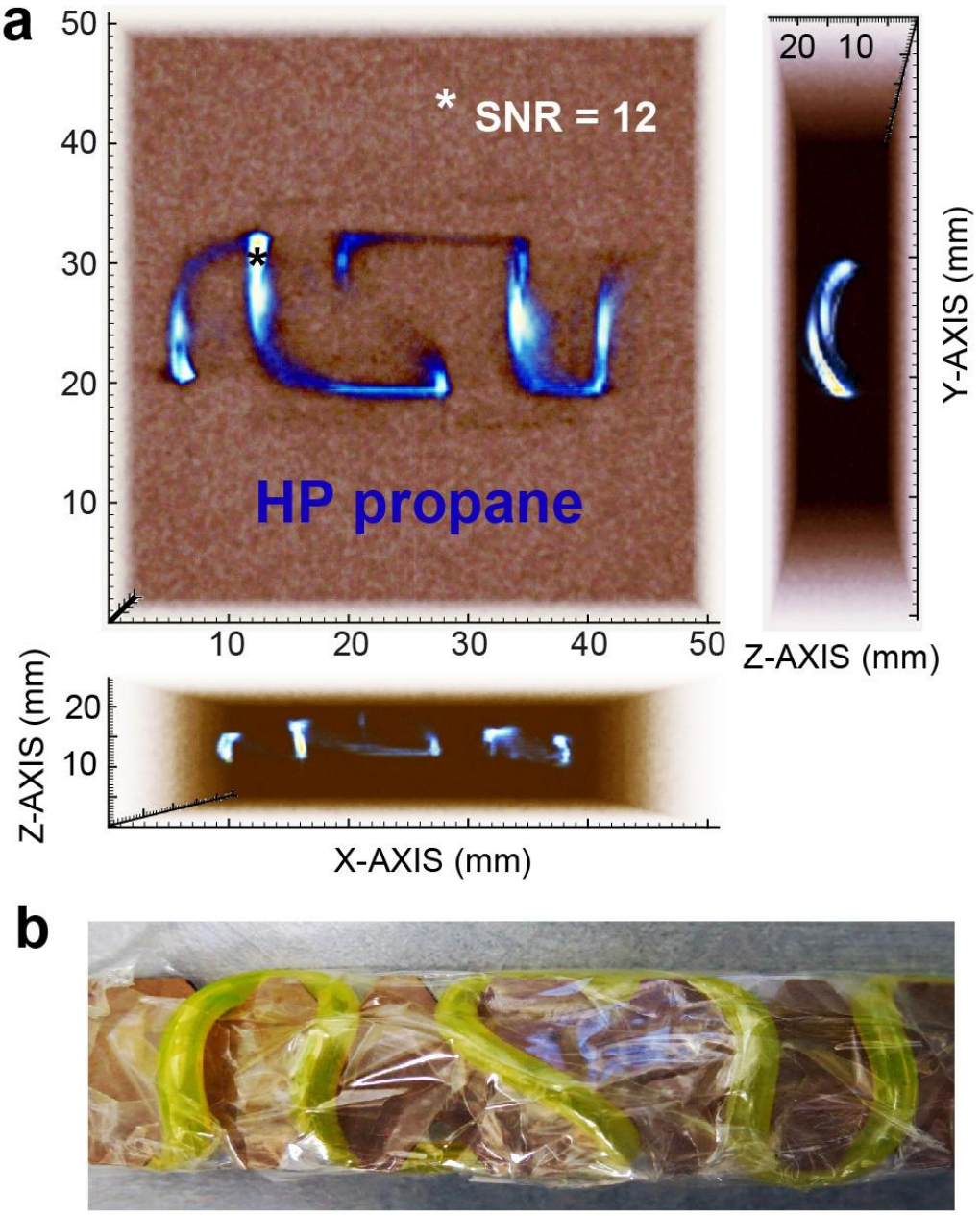

Figure S4. 3D gradient echo (GRE) ^{1}H MRI of flowing HP propane (a) in "NSU"-shaped phantom (Novosibirsk State University), with three projections shown. 3D image has voxel size of 0.8 × 0.8 × 0.8 mm^3 and the total imaging time of 17.4 s for acquisition of all 4096 individual lines in k-space with TR = 4.2 ms, TE = 2.1 ms, the field of view (FOV) 102.4 × 102.4 × 25.6 mm^3 and imaging matrix 128 ×128 × 32. A movie showing full 3D rendering is available in a separate SI. Varian's version of a 3D gradient echo (ge3D) was used with a total acquisition time of 17.4 s and a spectrum width (SW) of 40 kHz. The rf excitation pulse was Gaussian shaped pulse with 500 μs width (10° tipping angle). We note that in the MRI experiments the rf pulse was not spectrally selective. Therefore, both hyperpolarized signals of propane were excited. The emissive signal of the CH_3 group and the absorptive signal of the CH_2 group should be in anti-phase to each other immediately after the excitation pulse. However, because of the chemical shift difference they become partially in-phase at the maximum of the gradient echo. This prevents the complete mutual cancellation of the two contributions in the NMR signal and makes

the image detection possible. A thorough optimization of the pulse sequence can further improve the achieved SNR for HP propane imaging. b) A photograph of NSU shaped phantom. The phantom was constructed of Tygon™ (3/32 in. ID x 3/16 in. OD) tubing, wrapped around cardboard to construct the proper letter shapes and also to provide the phantoms with more depth to invoke better spatial dimensionality in the resulting image. Please note the apparent MRI signal losses in (a) in the areas of the phantom corresponding to those with the highest gas velocity along the x-axis. These MRI signal losses can be recovered by further decreasing the imaging acquisition time of the pulse sequence. Such decrease in acquisition time will also positively impact the TR and TE parameters by further accelerating MRI sequence. The MRI signal loss due to fast local gas flow is a potential limitation of the presented 3D MRI of the fast flowing gas. However, this limitation can be mitigated by (i) decreasing the overall gas flow and adjusting the imaging parameters, i.e. excitation pulse angle and TR/TE parameters, and (ii) by performing MRI of stopped gas. The latter will likely require careful synchronization with the MRI acquisition sequence, when the gas is stopped only during MRI encoding and MRI acquisition, and the hyperpolarized gas is allowed to flow during the rest of TR time period. This can certainly be accomplished on the millisecond time scale necessary for fast image acquisition.

Percentage hyperpolarization, enhancement factor and quantification of PHIP polarized propane gas at 4.7 T

Non-hyperpolarized sample is typically used as a signal reference for calculation of the signal (and polarization) enhancement factors. This is challenging for the spin system studied for two primary reasons: (i) only two (out of eight) protons in this spin system are being hyperpolarized via ALTADENA, and more importantly (ii) a 'true' signal reference has to be represented by a flowing propane gas with similar flow rate as the reaction mixture used. However, flowing propane (~15 mL/s) would not develop the full thermal polarization, because its exposure time to the magnetic field is short compared to T_1, i.e. the sample will not have sufficient time to reach equilibrium spin polarization. As a result, this approach[4] tends to significantly overestimate the achieved enhancement factor ε and %P. Performing quantification experiments with stopped gas may be non-ideal either for computing % polarization, because of potential gas leaks and other experimental factors that can also lead to overestimated values of ε and %P.

Here, an external signal reference sample was used for calculation of ε and %P as described earlier[5,6] using the following equations:

$$\varepsilon = \frac{S_{HP} \cdot [THERMAL]}{S_{THERMAL} \cdot [HP]}$$

and

$$\%P_{HP} = \varepsilon \cdot \%P_{THERMAL}$$

where S_{HP} is the integral of the NMR signal of hyperpolarized propane carrying two hyperpolarized protons; $S_{THERMAL}$ is the integrated NMR signal of water (with two thermally polarized protons) with equilibrium (thermal) level of polarization; [*THERMAL*] and [*HP*] are molar concentrations of reference (thermal) and hyperpolarized compounds respectively in the

phantom of the same volume. $\%P_{THERMAL}$ is equilibrium percentage polarization of proton nuclear spins at 4.7 T, i.e. $1.6 \bullet 10^{-5}$ or 0.0016%. We note that both HP propane (two HP protons/molecule) and thermally polarized water (2 protons/molecule) have equal number of protons relevant to calculation of the enhancement factor and percentage hyperpolarization. Reference spectrum of water and the spectrum of flowing HP propane recorded in the same phantom (i.e. identical volume) consisting of Tygon 3/32 in. ID tubing are shown in Fig. S5. This representative experiment yielded $S_{THERMAL}$ = 199.2 a.u. and S_{HP} = 57.4 a.u. [*THERMAL*] = 55 M, while the concentration of [*HP*] was calculated as follows:

$$[HP] = 0.5 \cdot \frac{1\ mole}{22.4\ L} \cdot \frac{273\ K}{300\ K} = 0.020\ M$$

where 273K/300K reflects the correction for deviation from normal conditions, 0.5 is the molar fraction of propane gas in the resulting mixture of HP propane:parahydrogen of ~1:1 assuming complete conversion of propene (Note if the conversion is incomplete, the [HP] is <0.020 M). The resulting enhancement factor ε was 792 ([57.4 a.u.•55 M]/[199.2 a.u.•0.020]) corresponding to $\%P_H$ = 1.3% (or 0.0013) per each (two per molecule) HP proton in ALTADENA hyperpolarized propane.

The detected % polarization of 1.3% is far from theoretical maximum of 100% (or unity), which can be explained by several factors: (i) parahydrogen gas used contained ~90-95% para-state, i.e. not 100%, (ii) T_1 relaxation losses during gas transportation from the reactor (Fig. 1a) to the rf coil of the MRI scanner, and most importantly (iii) a competing mechanism on non-pairwise addition of parahydrogen to propene. The latter can be potentially improved and lead to further significant gains in the detection sensitivity of HP propane gas.

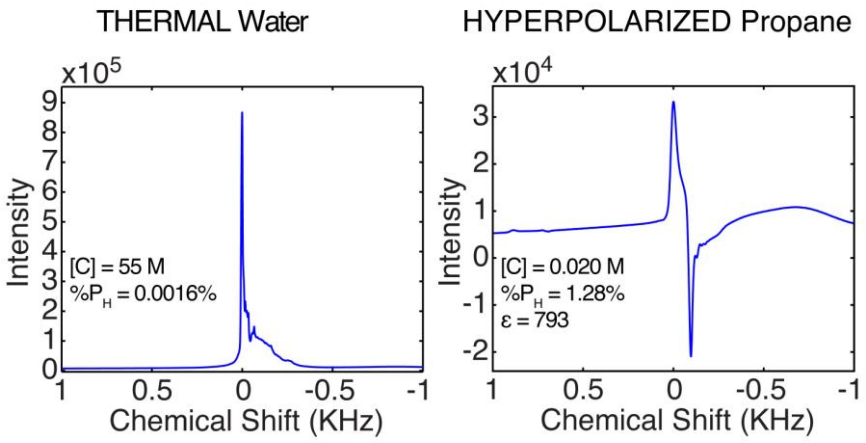

Figure S5. ^{1}H NMR spectroscopy of samples of thermally polarized liquid water (left) and flowing hyperpolarized (HP) propane gas (right) produced using Rh/TiO_2 catalyst and 1:2 molar ratio of propene:parahydrogen mix resulting in ~1:1 molar ratio HP propane:parahydrogen mixture during detection in 4.7 T pre-clinical MRI scanner. Both samples were studied in the same section of Tygon tubing (3/32 in ID). Single scan NMR spectra were acquired with 90° excitation RF pulse (~100 μs). The broad peak seen in the right spectrum at ~-0.7 kHz is proton background signal from the rf coil.

References used in Supporting Information (SI)

1. Patent 4983372 US. Process for preparing halide-free rhodium nitrate 08.01.91

2. J. Moudler, W. Stickle, P. Sobol, K. Bomben Handbook of X-ray Photoelectron Spectroscopy, Perkin-Elmer Corp.: Eden Priarie, MN, 1992.

3. M. G. Pravica, D. P. Weitekamp, *Chem. Phys. Lett.* **1988**, *145*, 255-258.

4. R. Sharma, L. S. Bouchard, *Sci Rep* **2012**, *2*, 5.

5. P. Nikolaou, A. M. Coffey, L. L. Walkup, B. Gust, C. LaPierre, E. Koehnemann, M. J. Barlow, M. S. Rosen, B. M. Goodson, E. Y. Chekmenev, *J. Am. Chem. Soc.* **2014**, *136* 1636–1642.

6. K. W. Waddell, A. M. Coffey, E. Y. Chekmenev, *J. Am. Chem. Soc.* **2011**, *133*, 97-101.